K. HASHIMOTO*, N. KUMAGAI**, K. IZUMIYA**, H. TAKANO**, P.R. ŻABIŃSKI*** ,
A.A. EL-MONEIM****, M. YAMASAKI*****, Z. KATO******, E. AKIYAMA*******, H. HABAZAKI********

THE USE OF RENEWABLE ENERGY IN THE FORM OF METHANE VIA ELECTROLYTIC HYDROGEN GENERATION

ZASTOSOWANIE ODNAWIALNEJ ENERGII W FORMIE METANU NA DRODZE ELEKTROLITYCZNEJ PRODUKCJI WODORU

Extrapolation of world energy consumption from 1990 to 2010 indicates the complete exhaustion of world reserves of oil, natural gas, uranium and coal by 2040, 2043, 2046 and 2053, respectively. For the survival of all people in the whole world, intermittent and fluctuating electricity generated from renewable energy should be supplied in the form of usable fuel to all people in the whole world. We have been working on research and development of global carbon dioxide recycling for the use of renewable energy in the form of methane via electrolytic hydrogen generation using carbon dioxide as the feedstock. We created energy-saving cathodes for hydrogen production, anodes for oxygen evolution without chlorine formation in seawater electrolysis, and catalysts for methanation of carbon dioxide and built pilot plants of industrial scale. Recent advances in materials are described. Industrial applications are in progress.

Keywords: Renewable energy, methane supply, CO_2 recycling, electrolytic hydrogen generation, CO_2 methanation, syngas methanation, fuel depletion, survival of world population

Ekstrapolacja światowego zużycia energii z lat 1990-2010 wskazuje, że całkowite wyczerpanie światowych zasobów ropy naftowej nastąpi w 2040 roku, gazu ziemnego w 2043 roku, uranu w 2046 roku a węgla w 2053 roku. Dla przetrwania ludzkości na całym świecie energia elektryczna powinna być generowana z odnawialnego źródła w formie paliwa dostępnego dla każdego. Opracowano technologię globalnego recyklingu dwutlenku węgla i zastosowania metanu jako formy odnawialnej energii generowanej poprzez uwodornienie CO_2 wodorem produkowanym podczas elektrolizy wody morskiej. Opracowano energooszczędne katody do produkcji wodoru, anody do produkcji tlenu bez towarzyszącej temu emisji gazowego chloru podczas elektrolizy wody morskiej oraz katalizatory stosowane w procesie uwodornienia dwutlenku węgla. Wybudowano również pilotażową instalację w skali przemysłowej. Praca opisuje ostatnie postępy w industrializacji procesu.

1. Future of Energy

We have been working on research and development (R&D) of a global CO_2 recycling system over the last two decades. Now the industrial applications of global CO_2 recycling are in progress. At first, let us identify problems in global energy in the current situation of unlimited access to energy resources, including oil, natural gas, coal, and uranium. The US Department of Energy (DOE) is posting energy-related world data over the period from 1980 mostly to 2010 including energy consumption, CO_2 emission, and population of individual areas of the globe in addition to the world reserves of oil, natural gas, and coal [1]. Figure 1 reproduces from the DOE data the chronological patterns of variation in energy consumption per capita over the 29-31 years in three groups

of countries as well as those of the world, Japanese, American and Chinese. The difference in the energy consumption per capita among countries is clear. Figure 2 shows the CO_2 emissions per capita. It is difficult at glance to distinguish Figs. 1 and 2 other than the different ordinates. The Kyoto Protocol concerning sustainability of the global environment was adopted in 1997. The Conference of Parties, COP 18, to the United Nations Framework Convention on Climate Change was held from November 26 to December 7, 2012 in Doha, Qatar, where the creation of a fair, effective and legal framework to which all countries can take part was discussed. However, there is no trend of decreasing energy consumption and carbon emissions per capita in developed countries except for temporary fluctuations influenced by economic situation. The energy consumption and carbon emissions per capita of

* PROFESSOR EMERITUS OF TOHOKU UNIVERSITY AND TOHOKU INSTITUTE OF TECHNOLOGY, TOHOKU INSTITUTE OF TECHNOLOGY, SENDAI, 982-8577 JAPAN

** DAIKI ATAKA ENGINEERING, CO., LTD., 11 SHINTOYOHUTA, KASHIWA, 277-8513 JAPAN

*** AGH UNIVERSITY OF SCIENCE AND TECHNOLOGY, FACULTY OF NON-FERROUS METALS, 30-059 KRAKÓW, 30 MICKIEWICZA AV., POLAND

**** EGYPT-JAPAN UNIVERSITY OF SCIENCE AND TECHNOLOGY, ALEXANDRIA, EGYPT

***** GRADUATE SCHOOL OF SCIENCE AND TECHNOLOGY, KUMAMOTO UNIVERSITY, 860-8555 JAPAN

****** DEPARTMENT OF ENVIRONMENT AND ENERGY, TOHOKU INSTITUTE OF TECHNOLOGY, SENDAI, 982-8577 JAPAN

******* NATIONAL INSTITUTE FOR MATERIALS SCIENCE, STRUCTURAL METALS CENTER, 305-0047 JAPAN

******** GRADUATE SCHOOL OF ENGINEERING, HOKKAIDO UNIVERSITY, SAPPORO, 060-0808 JAPAN

developing countries are far lower than those of developed countries. After Lehman Shock on September 2008, global economic recession drove energy consumption and carbon emissions lower, particularly in OECD countries and Eurasia. Oil, Natural gas, and coal consumption showed the bottom in 2009 but bounced back thereafter. Japan is exceptional. Because of earthquake, tsunami and nuclear accident, the energy consumption declined again in 2011. However, Japanese people have learned no inconvenience of cutting unnecessarily high lighting, heating and cooling, and hence the industrial activity as well as civic life has been kept with the lower level of energy consumption.
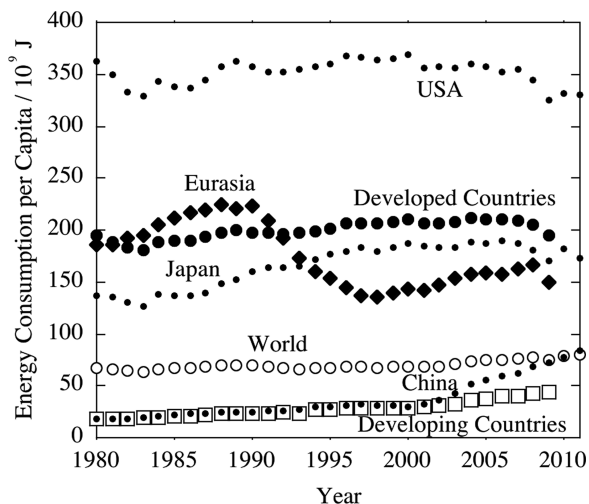

Fig. 1. Chronological patterns of variation in energy consumption per capita over a recent period of 29-31 years in three groups of countries as well as in the worldwide, Japan, the United States, and China [1]
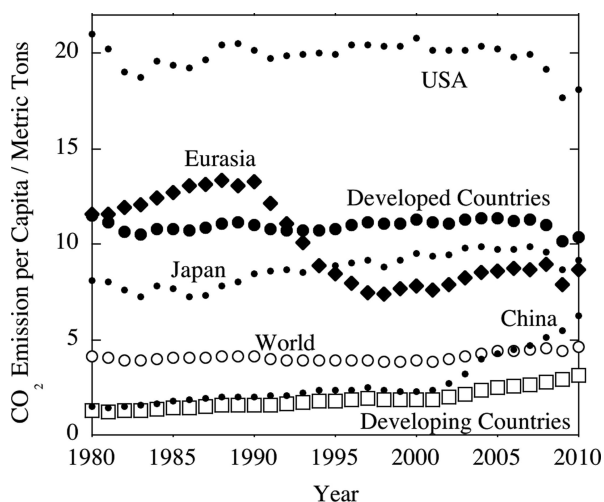

Fig. 2. Chronological patterns of variation in CO_2 emissions per capita over a recent period of 30 years in three groups of countries as well as in the worldwide, Japan, the United States, and China [1]

Figure 3 shows the energy consumption per capita for the three groups of countries in 2009 plotted against the population of the respective zone of the globe [1]. As mentioned above, the energy consumption in OECD countries and Eurasia was exceptionally lower in 2009. Nevertheless, the nearly a half of global energy consumption was spent by the developed countries in spite of the small proportion of populations

(17.8%), whereas the energy consumption of the developing countries, composing 78.0% of the global population, is just approaching to the level of developed countries. According to Fig. 3, residents in developing countries can double the current level of energy consumption per capita to reach the global average level of energy consumption per capita. In contrast, reduction of energy consumption per capita by 77% for US residents or by 56% for Japanese is desirable for these populations to reach the average global energy consumption level. Such a target is practically impossible to achieve. It is also impossible to reduce energy consumption per capita by nearly two-thirds in average for all developed countries and by one-half for Eurasian countries. Thus, it was inevitable that total world energy consumption would rise continuously.
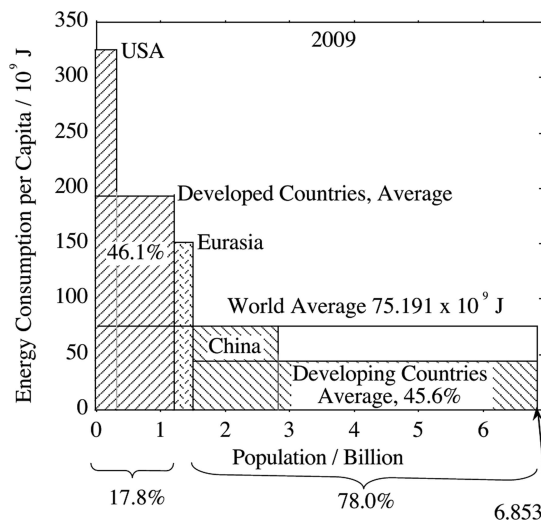

Fig. 3. Relationship between energy consumption per capita and population in the three groups of countries in 2009 [1]. Although the values of developed and developing countries include those of USA and China, respectively, the values of USA and China are separately overwritten

The left-hand-side of Fig. 4 shows the chronological patterns of global energy consumption for recent 30 years [1]. Annual global energy consumption increased steadily with a factor 1.020 from 1990 to 2010 after the collapse of the Soviet Union. The full line prediction curve in Fig. 3 was drawn by extrapolating the recent energy consumption record under the assumption of the annual rising factor of 1.020. In Fig. 4, the projected year of exhaustion is given under the assumption of the energy consumption mode in 2010: oil in 2040 and natural gas in 2043. If usage of uranium as the fuel for nuclear power reactors in any country is allowed without limitation, the estimated uranium resource of 5.33 Mt [2] will be exhausted in 2046. Then, in 2053, coal would be exhausted. There are some other estimates of world fossil fuel reserves, but the difference in estimates is not essential. If we adopt other data for fuel reserves, the projected years of exhaustion of fuels will be within few years from those estimated using DOE data. The minable years, that is the ratio of reserves to production in the year of production have often be expressed as the year of exhaustion of fuel reserves. However, the production should increase every year following the fuel demand. The world population showed a steadily rising from 1980 to 2010 with an annual increase of

80 million [1]. Provided that the trend of population rise holds at the current rate, global energy consumption per capita in 2050 will be 120×10^9 J year^{-1}, which is only about 60% of the average energy consumption per capita of the developed countries in 2009. Thus, the full line prediction in Fig. 4 may be underestimation. Even if new fossil fuel resources worth the oil reserves in 2009 are discovered, they are not sufficient to even supply to the energy demand from 2054 to 2060 in the empty space of Fig. 4. Continued use of fossil fuels will lead to intolerable global warming by the greenhouse effect. In fact, oil-producing countries should use the remaining oil for their own survival, and hence the oil supply will decline showing the maximum within 15-20 years. In fact, Indonesia declared on January 26, 2012, that they would place the priority for domestic oil consumption ahead of oil exportation.
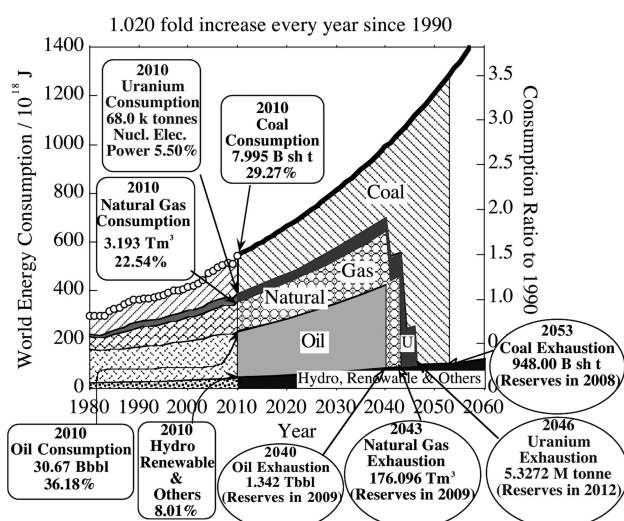

Fig. 4. Chronological patterns of variation in energy consumption over a recent period of 30 years [1] and future prospects of world energy demand estimated under the assumption of a continued rise in the rate of energy consumption evaluated over 1990 and 2010 and anticipated years of exhaustion of world reserves of fossil fuels [1] and uranium [2]

For the moment, the purchase of oil, natural gas, and coal, as well as uranium, has practically no trade limitation, and thus the incentive to develop urgently an economically viable system of renewable energy production remains low on account of low expectancy of immediate economic profit. However, looking straight at the reality that available fuel resources shall be exhausted around the middle of the 21st century and that the continued use of fossil fuels will lead to intolerable global warming, we need to establish the technologies to use renewable energy for all people in the whole world to survive and to spread the technologies to the whole world within next 15 years before the anticipated decline in the oil supply.

2. Difficulty in Usage of Renewable Energy

The renewable electric power excluding hydroelectric power in 2010 was only about 1.3 % of the world energy consumption. For the moment, renewable electric power generation systems have comparatively small output power and are integrated in the existing electricity supply network in a dispersed supplemental mode. However, for long-term sustained survival of human beings over the globe, we have to substitute the 100% energy consumption with renewable energy. There are sufficient renewable energy source on our planet. For example, in 2010, the total energy consumed worldwide was 517×10^{18} J year^{-1}. The corresponding amount of energy can be generated in the form of electricity by photovoltaic cells with an energy conversion efficiency of 15% in a desert area with solar intensity of 1000 Wm^{-2} operating for 8 h per day using a mere 2.04% of the area of the main deserts on the Earth. This estimate is rather encouraging us that we can survive on our planet.

The technologies of converting different types of renewable energy sources to electric power already exist. The inherent disadvantage of renewable energy sources in general is their instability with fluctuation with time. Thus, when electricity generated by renewable energy sources is integrated directly in the existing electricity supply network system, undesirable frequency fluctuation of supplied ac current is inevitable. In modern industry, ac electric power supply with a frequency fluctuation margin of ± 0.2 Hz is claimed to be unacceptable [3]. For example, when ac electricity with a frequency fluctuation margin exceeding ± 0.2 Hz is supplied to industrial plants manufacturing sheet products of steel and Al, product sheet has a varying thickness of unacceptable quality on account of fluctuation of rolling conditions or thickness fluctuation or even a cutting problem arises for a chemical textile or paper manufacturing plant. When such ac electric power with unstable frequency is used in an oil refinery, desulfurization is claimed to fail [3]. In Japan, the frequency fluctuation margin of ac electricity supplied to the customer is set at ± 0.2 Hz by all the electric power supply companies excluding Hokkaido Electric Power Company, which sets the margin at ± 0.3 Hz [3]. According to an estimate made by Hokkaido Electric Power Company [4], the frequency error margin of ± 0.3 Hz cannot be held when electricity generated by wind exceeds 250 MW (4.8% of the maximum total power in the net work). As such, it is difficult to integrate electricity generated by renewable energy sources with inherently fluctuating nature exceeding about 5% of the maximum instantaneous power output in the existing electricity supply grid. Thus, the electric energy generated by intermittent and fluctuating renewable sources should be converted in some form of fuel.

3. Global Carbon Dioxide Recycling

As early as the 1970s, we had been dreaming to supply hydrogen to all people in the whole world, generating hydrogen by seawater electrolysis using the renewable energy origin electricity. However, we understood that there are no infrastructure for mass transportation of hydrogen and no combustion technology for hydrogen. Thus, for realization of renewable-energy-fueled communities worldwide, we need to convert the energy generated by renewable energy sources to some form of fuel material for which the combustion technology as well as the mass transportation infrastructures have been established. More than two decades ago, the authors created a

catalyst that converted carbon dioxide CO_2 and hydrogen H_2 quickly to methane CH_4 with an almost 100% CH_4 selectivity [5]. Methane is the main constituent in natural gas, for which both the efficient mass transportation infrastructures and the combustion technologies have been well established. Thus, we proposed global CO_2 recycling on the basis of the discovery of this catalyst [6]. The sequence of energy conversion in the proposed system is as follows:

(i) Energy necessary for all people in the whole world is converted to electricity by photovoltaic cells in deserts.

(ii) The electricity is used for H_2 production by seawater electrolysis in plants installed along the coasts near the deserts.

(iii) H_2 is converted to CH_4 by the reaction with CO_2.

(iv) Using the available transportation infrastructure, the generated CH_4 is sent to the areas of consumption.

Only the difference from the current practice, CO_2 should be captured from the chimney and be sent to the place where the electricity is available from renewable energy. If this is realized we can use solar energy forever, using CO_2 as the feedstock without emitting in atmosphere.

Industrial technology for conversion of renewable energy sources to electricity is available and the infrastructures for CH_4 transportation and combustion technologies also exist. Recovery of CO_2 gas from chimney is also proved to be industrially viable. The properties of liquefied CO_2 are comparable to those of liquefied petroleum gas (LPG), and therefore, the transportation of the liquefied CO_2 is possible. Thus, the realization of the global CO_2 recycling can be performed by the establishment of the technologies to yield H_2 by seawater electrolysis and to produce CH_4 by the reaction of H_2 with CO_2.

4. Key Materials for Global Carbon Dioxide Recycling

Key materials toward realization of a global CO_2 recycling are a cathode and anode for seawater electrolysis and a catalyst for conversion of H_2 to CH_4 through the reaction with CO_2.

4.1. Cathode

We need the cathode consisting of inexpensive elements and having a high activity comparable of platinum black. We succeeded to create active and durable alloy cathodes by electrodeposition [7]. Key elements were iron and carbon. Figure 5 shows cathodic polarization curves of electrodeposited metals and alloys for hydrogen formation. Nickel is stable but less active. Iron is more active than nickel, and the Ni-Fe alloy is more active than iron. When iron and carbon are added to nickel, the activity becomes remarkably high, and is comparable of platinum black. The change in Tafel slope suggests that the hydrogen evolution on the Ni-Fe-C alloy cathodes is mechanistically fastest. We found that the significant charge transfer from nickel to iron by the addition of iron and carbon to nickel is responsible for remarkable acceleration of proton discharge to form hydrogen atoms adsorbed on the cathode surface and for change in the rate determining step from the generally very slow proton discharge to the generally fast formation of hydrogen molecule by combination of two hydrogen atoms adsorbed on the cathode surface.

The carbon addition was also effective to prevent corrosion of the cathode [8]. Figure 6 shows cathodic polarization curves of electrodeposited Co-Ni-Fe-C alloys for hydrogen formation. As an example of Co-18.1Ni-52.8Fe, the sufficient amount of iron addition to Co-Ni alloys significantly accelerates the hydrogen formation. However, when the shutdown period of electrolysis is lasted for 50 days without cathodic polarization, the beneficial effect of iron addition disappears because of loss of iron by dealloying corrosion in the hot alkaline solution during the shutdown period. When small amounts of carbon and iron are added, the alloy exhibits high activity for hydrogen production and no dealloying corrosion after open circuit immersion for 50 days in the hot alkaline solution.
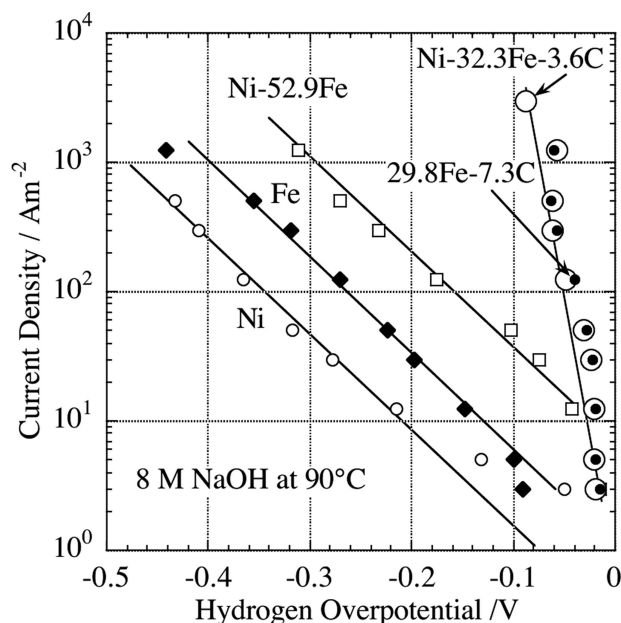

Fig. 5. Galvanostatic polarization curves of electrodeposited metals and alloys measured in 8 M NaOH solution at 90°C [7]
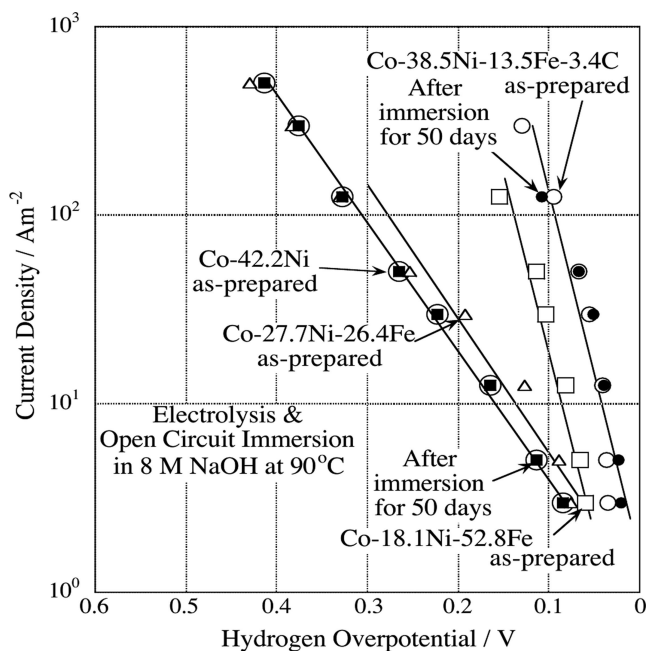

Fig. 6. Galvanostatic polarization curves measured in 8 M NaOH solution at 90°C for electrodeposited metals and alloys before and after immersion for 50 days in 8 M NaOH solution at 90°C [8]

These cathodes made of Ni-based alloys or Co-based alloys can be used not only for direct seawater electrolysis but also for high temperature alkali electrolysis.

4.2. Anode Materials for Seawater Electrolysis

Industrial electrolysis of NaCl solution in either the chlor-alkali industry or sodium hypochlorite (NaClO) production has been conducted for the formation of chlorine Cl_2 on the anode. However, in seawater electrolysis for massive amounts of H_2 production, the Cl_2 formation on the anode should be avoided. An anode material to form oxygen in place of Cl_2 by seawater electrolysis is required as in the case of fresh water electrolysis. This concern has been solved by developing special anode bearing single phase multiple oxides consisting mainly of Mn containing also Mo, W, Sn, and/or Fe as active electrocatalysts [9-12].

The developed anode was composed of three layers: Ti substrate, conductive oxide intermediate layer such as IrO_2 for prevention of growth of insulating TiO_2 by anodic oxidation of the Ti substrate, and electrocatalyst consisting of single phase multiple oxides to form oxygen without forming Cl_2. The electrocatalyst is prepared by anodic deposition on the DSA-type anode in $MnSO_4$ solutions containing other necessary cations.

During prolonged service use of such a three layer anode possessing an intermediate layer such as IrO_2 with heterogeneous thickness for electrolysis of seawater, the local destruction of electrocatalyst and intermediate layers takes place by the localized oxide growth on the Ti substrate surface at the thinner part of the intermediate layer, where inward diffusion of oxygen through the intermediate layer to reach the Ti substrate is easier. This leads to the termination of the anode life by Cl_2 evolution at such locally destroyed spots of the anode. The intermediate IrO_2 layer was prepared as follows: brushing application of H_2IrCl_6 butanol solution over the Ti substrate surface; drying at 80°C in air and then calcination at 450°C in air; repeating the above three steps three times. On account of high viscosity of the H_2IrCl_6 butanol solution, it is difficult to prepare the IrO_2 layer with homogeneous thickness. Thus, localized destruction of the electrocatalyst and intermediate layers tends to proceed at the thinner part of the IrO_2 intermediate layer due to localized growth of TiO_2 bumps. IrO_2 as well as SnO_2 has a rutile structure. Thus, in place of IrO_2, a single phase $Sn_{1-x}Ir_xO_2$ double oxide layer with homogeneous thickness has been prepared as the intermediate layer over the Ti substrate by brushing application of a H_2IrCl_6-$SnCl_4$ butanol solution. Figure 7 shows a comparison of the performance of the oxygen evolution anode consisting of thin $Sn_{1-x}Ir_xO_2$ double oxide intermediate layer with that of thin IrO_2 intermediate layer [13]. On account of heterogeneity of the IrO_2 intermediate layer, the oxygen evolution efficiency of the anode with the thin IrO_2 intermediate layer coated using a 0.1 M H_2IrCl_6 butanol solution without $SnCl_4$ dropped down to 96% by electrolysis for only 40 min in a 0.5 M NaCl solution. In contrast, the anode life exceeding 4200 h has been realized in a 0.5 M NaCl solution with the $Sn_{1-x}Ir_xO_2$ intermediate layer.

Even if a uniform intermediate layer is formed the inward diffusion of oxygen through the oxide electrocatalyst and the oxide intermediate layer is unavoidable, and hence during electrolysis the insulating titanium oxide grows gradually with a consequent increase in the electric resistivity of the anode. This leads to the increase in the cell voltage of electrolysis.

Consequently, for seawater electrolysis using oxide anode for oxygen evolution in seawater electrolysis, it is essential to develop some effective barrier against inward diffusion of oxygen through the oxide layers to the Ti substrate surface. Furthermore, use of rare element, Ir, in the form of IrO_2 for the intermediate layer of the anode is certainly not acceptable for industrial large-scale seawater electrolysis facilities, although it is acceptable for a laboratory experiment. Thus, development of an economically viable anode material still remains a serious challenge.
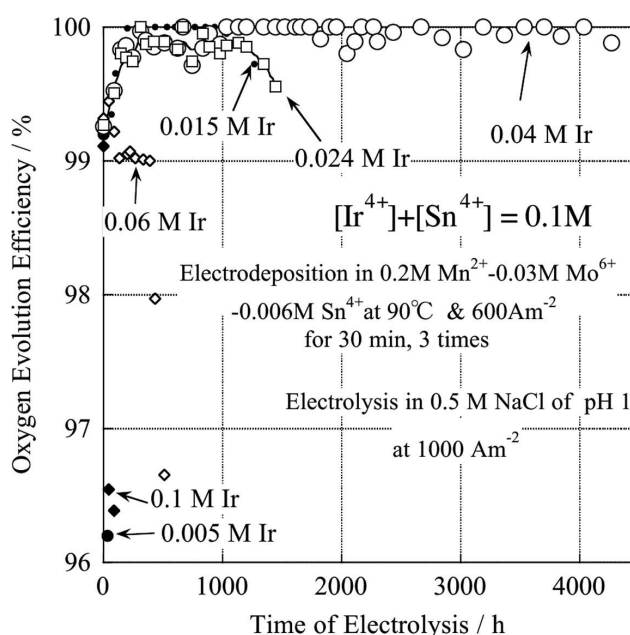

Fig. 7. Dependence of oxygen evolution efficiency at current density of 1000 Am^{-2} in 0.5 M NaCl solution at pH 1 on duration of electrolysis for the anodes consisting of $Mn_{1-x-y}Mo_xSn_yO_{2+x}$ electrocatalyst prepared by anodic deposition for 30 min, 3 times over IrO_2 and $Sn_{1-x}Ir_xO_2$ intermediate layers [13]. Intermediate IrO_2 layer was prepared from 0.1 M H_2IrCl_6 butanol solution, and $Sn_{1-x}Ir_xO_2$ layers were prepared from butanol solutions in which the sum of H_2IrCl_6 and $SnCl_4$ was 0.1 M

Direct seawater electrolysis for generation of hydrogen is certainly a clean option of acquiring an energy source, but there are numerous technical problems to be solved to realize electrolysis of neutral seawater with no buffer action using an oxide electrode without forming undesired Cl_2. In terms of energy consumption at present, this direct seawater electrolysis cannot compete against high temperature alkali electrolysis undertaken for desalinated seawater. Thus, at the moment, for a large-scale industrial plant, high temperature alkali electrolysis is preferred to direct seawater electrolysis.

4.3. Methanation of Carbon Dioxide

4.3.1. Catalyst for CO_2 Methanation

Our objective is to form CH_4 very rapidly by the reaction of CO_2 with H_2 without forming the toxic by-product such as CO through the reaction

$$CO_2 + 4H_2 \rightarrow CH_4 + 2H_2O. \qquad (1)$$
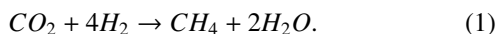
When we used amorphous Ni-Zr alloys as the catalyst precursor for the reaction of CO_2 with H_2, CO_2 conversion rapidly occurred with an almost 100% CH_4 selectivity in the temperature range of 200-300°C according to Eq. (1) [5]. When the amorphous Ni-Zr alloy catalyst precursor is exposed to a $CO_2 : H_2 = 1 : 4$ mixture at a temperature in the range of 200-300°C, zirconium is oxidized selectively and converted to ZrO_2, while nickel remains in the metallic state, with a consequent formation of the catalyst consisting of nickel supported on ZrO_2. Such a catalyst can be produced practically from the amorphous Ni-Zr alloy precursor through oxidation in air and subsequent reduction in a H_2 atmosphere. At around the catalytic reaction temperature of 200-300°C, the thermodynamically stable phase of ZrO_2 is monoclinic, but a considerable fraction of tetragonal ZrO_2 has been found from the amorphous Ni-Zr precursor, and Ni supported on tetragonal ZrO_2 has possessed a high catalytic function [14]. The tetragonal ZrO_2 has been identified as the double oxide in which at the formation of ZrO_2 lattice by oxidation of zirconium in Ni-Zr alloys Ni^{2+} ions have also been included occupying the lattice points of ZrO_2 lattice. Thus, the higher the nickel content in the amorphous Ni-Zr precursor, the higher is the fraction of tetragonal ZrO_2 type double oxide and the higher is the catalytic activity [15]. However, when the nickel content of the Ni-Zr precursor is excessively high, unfavorable nickel agglomeration proceeds over the catalyst surface and leads to a loss of the active site of catalyst, that is, nickel atoms on the surface of the ZrO_2 type double oxide. Thus, it is not straightforward to gain enhanced catalytic activity of the Ni/tetragonal ZrO_2 type double oxide catalyst through a simple rise of the nickel proportion in the amorphous Ni-Zr precursor.

It is ideal if the fraction of the tetragonal ZrO_2 type oxide rises without increasing the proportion of nickel in the amorphous Ni-Zr precursor. It is known empirically that the tetragonal ZrO_2 type double oxide is stabilized by partial replacement of Zr^{4+} with metal ions with lower valence like trivalent rare earth elements and divalent Ca^{2+} and Mg^{2+} as well as Ni^{2+}. In fact, we managed to raise the catalytic activity of the Ni/tetragonal ZrO_2 type oxide catalyst by adding rare earth elements to the amorphous Ni-Zr precursor [16]. We [17] also demonstrated that the developed catalyst from the amorphous Ni-Zr-Sm precursor promoted methanation of CO preferentially for a gas mixture of CO, CO_2 and H_2.

4.3.2. The characterization of Catalyst and CO_2 Methanation Mechanism

Let us review briefly why the tetragonal ZrO_2 type oxide is effective as a catalyst for the CO_2 methanation by the reaction with H_2. It has been known [18] that the adsorption capacity of CO_2 is more than one order of magnitude higher and that of CO is a factor of 5–10 higher for monoclinic ZrO_2 than for tetragonal ZrO_2. Thus, upon formation of methanol CH_3OH from CO_2 or CO, since the rate of this reaction is controlled by adsorption of CO_2 or CO on the catalyst, the rate of CH_3OH formation is reported to be a factor of 4.5 faster for CO_2 or a factor of 7.5 faster for CO with Cu/monoclinic ZrO_2 catalyst than with Cu/tetragonal ZrO_2 [19]. In contrast,

the catalytic activity of our catalyst for CH_4 formation from CO_2 or CO is far lower for monoclinic ZrO_2 than for tetragonal ZrO_2. Thus, we can conclude that the rate-determining step for CH_4 formation from CO_2 and CO is not the process of adsorption of CO_2 and CO on our catalyst. We observed that, for enhancing the methanation efficiency of CO_2 and CO, partial replacement of Zr^{4+} with metal ions having a smaller valence than Zr^{4+} in the tetragonal ZrO_2 type double oxide was favorable. This can be interpreted in terms of increased oxygen vacancies by an increased proportion of Zr^{4+} replaced with lower valent metal ions, leading to a certain mode of deformation of close-packed oxygen lattice and making the tetragonal lattice more stable than the monoclinic lattice. The introduced oxygen vacancies by partial replacement of Zr^{4+} with lower valent metal ions interact strongly with oxygen in the surrounding environment. For example, upon heating of tetragonal ZrO_2 stabilized with Y^{3+} in air containing water steam at 250°C, H_2O was absorbed in the amount equivalent to the amount of oxygen vacancies, judging from the mass change, and led to phase transformation of the ZrO_2 double oxide to monoclinic ZrO_2 [20]. On account of strong interaction of oxygen vacancies in the ZrO_2 double oxide with oxygen in the environment such as oxygen in CO and CO_2 as well as in H_2O, the C=O bond in CO_2 or CO would become weaker under the presence of the ZrO_2 double oxide catalyst to promote direct reaction of CO_2 and CO to form CH_4 and H_2O. Our recent kinetic study [21] suggested that the rate-determining step of methanation of CO_2 is a splitting process of two oxygen atoms from CO_2 to form an active carbon atom and two water molecules due to strong interaction of oxygen in CO_2 with the oxygen vacancies in the catalyst surface.

4.3.3. Catalyst for Mass Production

As reviewed above, it was verified by laboratory investigation that nickel supported on the tetragonal ZrO_2 type double oxide formed from the amorphous Ni-Zr alloy precursors was the efficient catalyst for CO_2 methanation. However, in general, amorphous alloys are not suitable for mass production of industrial catalyst. As mentioned above, the essential factor for high catalytic activity for CO_2 methanation is not the amorphous structure but the presence of the tetragonal ZrO_2 type multiple oxide containing extra cations with lower valence than Zr^{4+}. Thus, we synthesized the tetragonal ZrO_2 type double oxide by calcination of a mixture of zirconia hydrosol with a salt of rare earth elements and then by impregnation of nickel on the tetragonal ZrO_2 type double oxide. The catalyst thus prepared was proved to act satisfactorily as a catalyst for CO_2 methanation [22].

Aiming at further simplification of the catalyst preparation process, we calcined a mixture of zirconia hydrosol, rare earth element salt, and nickel salt to get a mixture of the tetragonal ZrO_2 type triple oxide and NiO. Then, surface NiO was reduced by H_2 to prepare metallic nickel supported on the tetragonal ZrO_2 type oxide. Figure 8 [23] plots the CO_2 conversion efficiency of 50 at.% Ni-50 at.% $(Zr_{0.833}Sm_{0.167})$ catalysts at different methanation temperatures as a function of calcination temperature. Methanation reaction is exothermic. Irrespective of the calcination temperature of catalyst, the CO_2

conversion efficiency at atmospheric pressure is detected to be the highest at the methanation temperature of 350°C. At further higher temperatures because of reverse reaction the methanation efficiency declines. At any methanation temperature, the CO_2 conversion efficiency appears to be the highest with the catalyst calcined at 650-800°C. The reason for this shall be discussed later in the text.
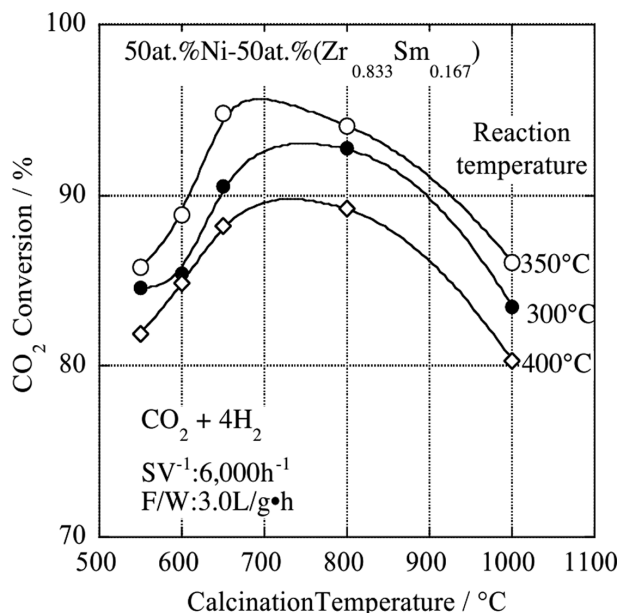

Fig. 8. Change in CO_2 conversion efficiency to form CH_4 on 50 at.% Ni-50 at.% ($Zr_{0.833}Sm_{0.167}$) catalyst with calcination temperature and reaction temperature [23]
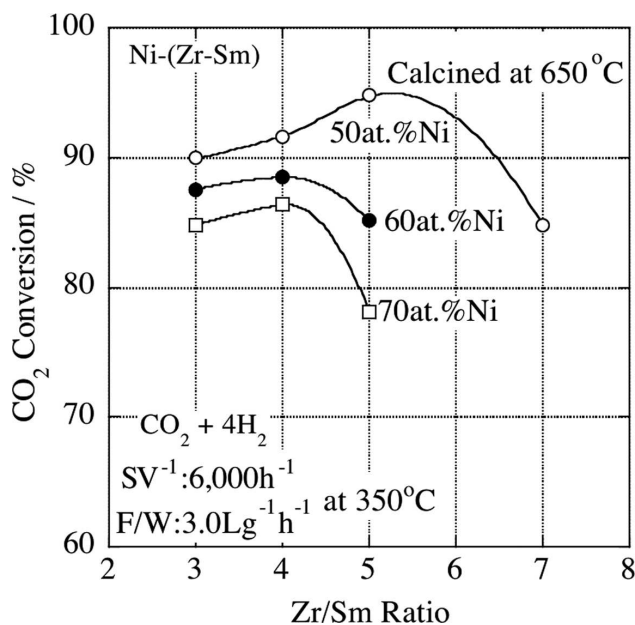

Fig. 9. Change in CO_2 conversion efficiency to form CH_4 on Ni-Zr-Sm catalysts with Zr/Sm ratio and catalyst composition [23]

Figure 9 [23], shows the dependence of CO_2 conversion efficiency on Zr/Sm mole ratio in the Ni/tetragonal $Zr_{1-x-y}Sm_xNi_yO_{2-0.5x-y}$ triple oxide catalysts at three different ratios of Ni/(Zr+Sm). The 50 at.% Ni-50 at.% (Zr-Sm) shows the highest activity for CO_2 methanation at any Zr/Sm ratio. The addition of excessive Ni (60 or 70%) lowers the methanation efficiency due to a decrease in the ZrO_2 type ox-

ide. Although not plotted in Fig. 9, the methanation efficiency was also lower by decreasing the nickel content to 40% on account of a decrease in active surface nickel atoms. Thus, 50 at.% Ni-50 at.% (Zr-Sm) must have been the optimum catalyst composition. At a given calcination temperature of 650°C, the catalytic activity of Ni/tetragonal $Zr_{1-x-y}Sm_xNi_yO_{2-0.5x-y}$ triple oxide catalysts appears to rise with increasing Zr/Sm ratio due to an increase in the tetragonal $Zr_{1-x-y}Sm_xNi_yO_{2-0.5x-y}$ triple oxide, although an excessively high Zr/Sm ratio is detrimental to the catalytic function on account of lower amount of oxygen vacancies due to a decrease in samarium in the tetragonal $Zr_{1-x-y}Sm_xNi_yO_{2-0.5x-y}$ triple oxide.

Thus, the CO_2 methanation efficiency of the Ni-(Zr-Sm) catalyst is dependent on the Ni/(Zr-Sm) ratio, Zr/Sm ratio, and calcination temperature, and changes with the fraction of the tetragonal ZrO_2 type triple oxide and with the proportions of samarium and nickel in the tetragonal ZrO_2 type triple oxide which determine the amount of oxygen vacancies.

Figure 10 [23] shows the variation of the 101 lattice spacing of tetragonal $Zr_{1-x-y}Sm_xNi_yO_{2-0.5x-y}$ triple oxides with varying the Zr/Sm ratio as a function of calcination temperature. The 101 lattice spacing for a given Zr/Sm ratio and at a given nickel content rises monotonically with rising calcination temperature. At a given Zr/Sm ratio, the 101 lattice spacing is smaller when $Zr_{1-x-y}Sm_xNi_yO_{2-0.5x-y}$ triple oxide contains higher amounts of Ni^{2+} at 70% Ni than at 50% Ni. The 101 lattice spacing expands with increasing Sm content in the $Zr_{1-x-y}Sm_xNi_yO_{2-0.5x-y}$ triple oxide by decreasing Zr/Sm ratio. The ionic radii are 0.0964 nm for Sm^{3+}, 0.079 nm for Zr^{4+}, and 0.069 nm for Ni^{2+}. Thus, the 101 lattice spacing is the smallest for the 70% Ni catalyst with the highest Zr/Sm ratio (70–5) and that, when compared at the same calcination temperature, the 101 lattice spacing rises with increasing samarium content by decreasing the Zr/Sm ratio from 5 to 3 and with decreasing nickel content from 70 to 50 at.%.
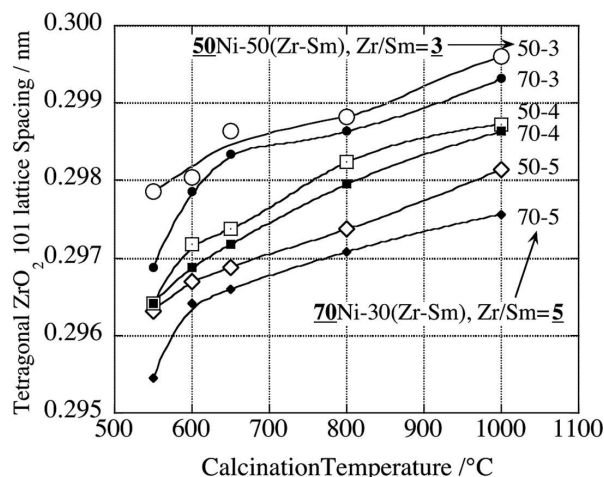

Fig. 10. Change in the 101 lattice spacing of tetragonal $Zr_{1-x-y}Sm_xNi_yO_{2-0.5x-y}$ triple oxide of Ni-(Zr-Sm) catalysts with calcination temperature [23]

The expansion of the 101 lattice spacing with rising calcination temperature for given ratios of Ni/(Zr+Sm) and Zr/Sm in Fig. 10 can be interpreted in terms of increasing proportion of uptake of samarium from the surrounding amorphous phase in the tetragonal $Zr_{1-x-y}Sm_xNi_yO_{2-0.5x-y}$ triple oxide with a

resultant increase in oxygen vacancies. The increase in the methanation efficiency with rising calcination temperature for 50 at.% Ni-50 at.% $Zr_{0.833}Sm_{0.167}$ catalysts as shown in Fig. 8 is ascribable to the increased number of oxygen vacancies in the tetragonal $Zr_{1-x-y}Sm_xNi_yO_{2-0.5x-y}$ crystal lattice. Thus, the rising calcination temperature is effective toward the enhancement of catalytic activity of the tetragonal ZrO_2 type triple oxide for the CO_2 methanation through the increase in the oxygen vacancies in the triple oxide lattice.

However, when the calcination temperature is excessively high (e.g., 1000°C), the CO_2 conversion efficiency decreases significantly as seen in Fig. 8. As shown in Fig. 11 [23] the crystal grain size of the tetragonal ZrO_2 type triple oxide increases linearly with rising calcination temperature. As shown in Fig. 12 [23], the BET surface area, hydrogen uptake and metal dispersion decrease with rising calcination temperature for the Ni-$(Zr_{0.833}Sm_{0.167})$ catalysts, resulting in worsening of the catalytic activity [23]. Consequently, rising calcination temperature for the Ni-Zr-Sm catalyst increases the catalytic activity through the increased proportion of elements stabilizing the tetragonal structure and the resultant increase in oxygen vacancies but diminishes density of active sites on the surface. Thus, the optimum calcination temperature for the Ni-Zr-Sm catalyst falls in the range of 650–800°C (Fig. 8). In the case of Ni-Zr-Sm, the optimized catalyst constitution is that the concentration of oxygen vacancies in ZrO_2 type oxide, that is, $Zr_{1-x-y}Sm_xNi_yO_{2-0.5x-y}$ in the Ni-Zr-Sm catalysts is as high as possible with the fine dispersion of nickel atoms over the surface of the ZrO_2 type oxide.

Fig. 12. Change in BET surface areas, hydrogen uptake and metal dispersion of 50 at.% Ni-50 at.% $(Zr_{0.833}Sm_{0.167})$ and 70 at.% Ni-30 at.% $(Zr_{0.833}Sm_{0.167})$ catalysts with calcination temperature [23]

In this connection, use of rare elements such as rare earth elements is not favorable for supply of fuel to the whole world. Instead of rare earth elements the stabilization of the tetragonal ZrO_2 type multiple oxide is realized by the addition of Ca^{2+} or Mg^{2+}. The CO_2 methanation activity of the best Ni-Zr-Ca catalyst prepared by calcination of a mixture of zirconia hydrosol with $CaSO_4$ and $NiSO_4$ has been found to be higher than that of the best Ni-Zr-Sm catalyst [24].

5. Toward Industrialization of Global Carbon Dioxide Recycling

Based on the successful developments of key materials we installed a prototype plant of global carbon dioxide recycling consisting of photovoltaic cell, an electrolyzer, a CO_2 methanation system, and a CH_4 combustor from which CO_2 is sent back to the CO_2 methanation system, over the rooftop of the Institute for Materials Research, Tohoku University in 1995. This small scale plant verifies that, as far as solar energy is available, in global CO_2 recycling, we can use solar energy at distant combustion system in the form of CH_4 and do not emit CO_2 in atmosphere but can use CO_2 repeatedly as the feedstock.

In 2003, a pilot plant of industrial scale has been installed at the Tohoku Institute of Technology that was capable of generating H_2 at a rate of 4 m^3h^{-1} and CH_4 at a rate of 1 m^3h^{-1}.

The basic technologies for realization of global CO_2 recycling are already in our hands. However, natural gas is readily available as a primary energy source nowadays but our methane is a quaternary energy formed by conversion three times from solar energy via. electricity and hydrogen. Every conversion requires cost, and hence our methane cannot compete with natural gas at present. However, as pointed out at the beginning of this review, exhaustion of energy resources on the Earth is inevitable in the foreseeable future. Indonesia government declared that they will refrain oil export to supply oil to the domestic demand. It is anticipated that, in 15–20 years, countries possessing oil resources will start imposing limitations on exports of their resources for their own survival. To face this severe reality straightforwardly, we have to
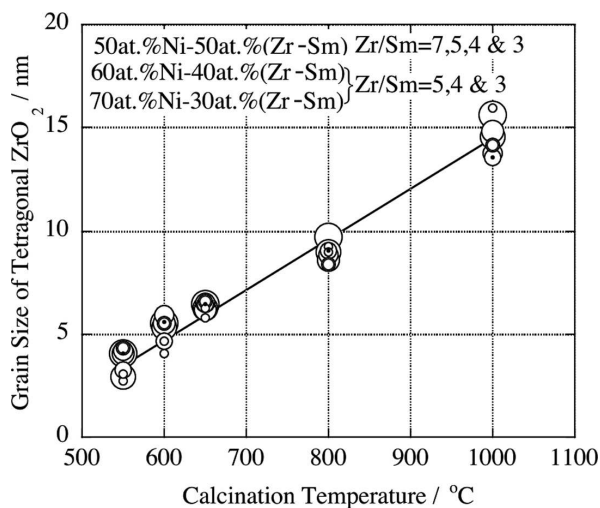

Fig. 11. Change in grain size of tetragonal $Zr_{1-x-y}Sm_xNi_yO_{2-0.5x-y}$ crystal in Ni-(Zr-Sm) catalysts evaluated from full width at half maximum of the 101 reflection in X-ray diffraction with calcination temperature [23]

In conclusion, the proposed procedure starting from calcination of a mixture of zirconia hydrosol, Ni salt, and a salt of cation stabilizing the tetragonal ZrO_2 structure to form oxide mixture of NiO and tetragonal ZrO_2 type multiple oxide and final reduction of surface NiO to form metallic nickel on the surface is ideal and promising for mass production of the desired catalyst for CO_2 methanation.
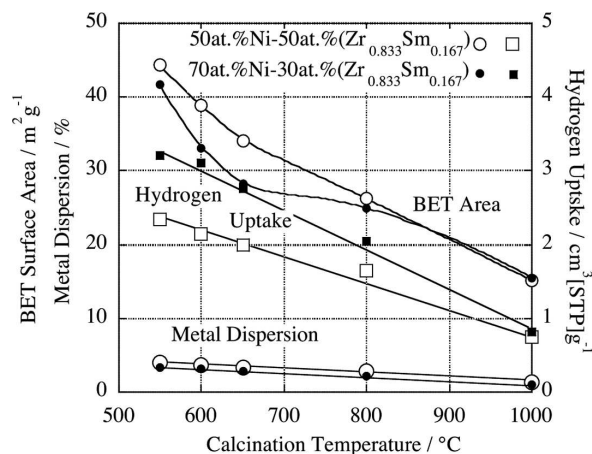
develop alternative means to acquire energy on a large scale to sustain continued prosperity of society. To the authors' knowledge, the proposed global CO_2 recycling system is the most convenient alternative to acquire massive amounts of energy from renewable resources without being dependent of fossil or fissile mineral resources.

The authors continue to invest research efforts to improve key materials and systems in the global CO_2 recycling system and to develop a large-scale industrial plant based on this concept. The task for scaling up the system to industrial dimension is not at all easy, but it is certainly not too early to start developing an industrial scale CO_2 recycling system. Furthermore, we have been performing to get the maximum amount of methane from biomass by a combination of CO and CO_2 methanation and water-gas shift reaction of biomass origin syngas on our catalyst [25].

Performing such efforts, the authors feel that the time is approaching for the global community to survive using renewable energy sources alone and be independent of fossil and fissile energy resources on the Earth.

REFERENCES

[1] http://www.eia.gov/tools/a-z/index.cfm

[2] http://www.world_nuclear.org/info/inf75.html

[3] http://www.re-policy.jp/keito/2/030912_09.pdf#search

[4] http://www.re-policy.jp/keito/2/030912_06.pdf#search

[5] H. Habazaki, T. Tada, K. Wakuda, A. Kawashima, K. Asami, K. Hashimoto, "Corrosion, Electrochemistry and Catalysis of Metastable Metals and Intermetallics", C. R. Clayton and K. Hashimoto Eds., the Electrochemical Society, 393-404 (1993).

[6] K. Hashimoto, Kinzoku (Materials Science & Technology), AGNE Gijutsu Center, Tokyo **63** [7], 5-10 (1993).

[7] S. Meguro, T. Sasaki, H. Katagiri, H. Habazaki, A. Kawashima, T. Sakaki, K. Hashimoto, J. Electrochem. Soc. **147**, 3003-3009 (2000).

[8] P.R. Żabiński, S. Meguro, K. Asami, K. Hashimoto, Mater. Trans. **44**, 2350-2355 (2003).

[9] K. Izumiya, E. Akiyama, H. Habazaki, N. Kumagai, A. Kawashima, K. Hashimoto, Electrochimica Acta **43**, 3303-3321 (1998).

[10] K. Fujimura, K. Izumiya, A. Kawashima, H. Habazaki, E. Akiyama, N. Kumagai, K. Hashimoto, J. Appl. Electrochem. **29**, 765-771 (1999).

[11] N.A. Abdel Ghany, N. Kumagai, S. Meguro, K. Asami, K. Hashimoto, Electrochimica Acta. **48** , 21-28 (2002).

[12] A.A. El-Moneim, N. Kumagai, K. Asami, K. Hashimoto, ECS Trans. **1**[4], 491-497 (2006).

[13] Z. Kato, N. Kumagai, K. Izumiya, K. Hashimoto, Appl. Surf. Sci. **257**, 8230-8236 (2011).

[14] M. Yamasaki, H. Habazaki, T. Yoshida, E. Akiyama, A. Kawashima, K. Asami, K. Hashimoto, Appl. Catal. A, General, **163**, 187-197 (1997).

[15] M. Yamasaki, H. Habazaki, T. Yoshida, M. Komori, K. Shimamura, E. Akiyama, A. Kawashima, K. Asami, K. Hashimoto, Studies in Surf. Sci. Catal. **114**, 451-454 (1998).

[16] H. Habazaki, T. Yoshida, M. Yamasaki, M. Komori, K. Shimamura, E. Akiyama, A. Kawashima, K. Hashimoto, Studies in Surf. Sci. Catal. **114**, 261-266 (1998).

[17] H. Habazaki, M. Yamasaki, B.-P. Zhang, A. Kawashima, S. Kohno, T. Takai, K. Hashimoto, Appl. Catal. A, General **172**, 131-140 (1998).

[18] K. Pokrovski, K.T. Jung, A.T. Bell, Langmuir, **17** [14], 4297-4303 (2001).

[19] K.T. Jung, A.T. Bell, Catalysis Letters, **80** [1-2], 63-68 (2002).

[20] N. Narita, Database of Grants-in-Aid for Scientific Research, Japan, http://kaken.nii.jp/ja/p/63550474/1988/3/ja

[21] H. Takano, K. Izumiya, N. Kumagai, H. Habazaki, K. Hashimoto, to be submitted.

[22] H. Habazaki, M. Yamasaki, A. Kawashima, K. Hashimoto, Appl. Organometallic Chem. **14**, 803-808 (2000).

[23] H. Takano, K. Izumiya, N. Kumagai, K. Hashimoto, Appl. Surf. Sci. **257**, 8171-8176 (2011).

[24] H. Takano, K. Izumiya, N. Kumagai, H. Habazaki, K. Hashimoto, to be submitted.

[25] H. Takano, H. Shinomiya, K. Izumiya, N. Kumagai, H. Habazaki, K. Hashimoto, to be submitted.